

Synthesis of Heterocyclic Ligands by Diheterocyclization at the Rhenium(I) Allenylidene [(triphos)(CO)₂Re{C=C=CPh₂}}](OSO₂CF₃). 1. Reactivity with Dipolar N,N-Heterocycles

Nicoletta Mantovani,[†] Paola Bergamini,[†] Andrea Marchi,[†] Lorenza Marvelli,^{*,†} Roberto Rossi,[†] Valerio Bertolasi,[‡] Valeria Ferretti,[‡] Isaac de los Rios,^{||} and Maurizio Peruzzini^{*,§}

Laboratorio di Chimica Nucleare ed Inorganica and Centro di Strutturistica Diffraattometrica, Dipartimento di Chimica, Università di Ferrara, Via L. Borsari 46, 44100 Ferrara, Italy, Istituto di Chimica dei Composti Organo Metallici, ICCOM CNR, Via Madonna del Piano 10, Area di Ricerca del CNR, 50019, Sesto Fiorentino, Italy, and Departamento Química Inorganica, Facultad de Ciencias, Campus Rio San Pedro, University of Cadiz, 11500 Puerto Real (Cadiz), Spain

Received August 2, 2005

1,2,3-Diheterocyclizations at the allenylidene ligand in the complex [(triphos)(CO)₂Re{C=C=CPh₂}}]-OTf (**1**; triphos = MeC(CH₂PPh₂)₃, OTf = OSO₂CF₃) readily occur upon reacting **1** with N,N-heterocycles such as 1*H*-benzotriazole, 2-aminopyridine, and 2-aminothiazole. The reaction of **1** with 1*H*-benzotriazole leads to [(triphos)(CO)₂Re{C=C(H)C(Ph)}]N(C₆H₄N=N)}OTf (**4**). Deprotonation of **4** with sodium methoxide in tetrahydrofuran at room temperature yields the alkynyl derivative [(triphos)(CO)₂Re{C≡CC(Ph)₂(NC₆H₄N=N)}] (**5**) via ring opening of the triazaindenyl moiety in **4**. Reaction of **1** with 2-aminopyridine or 2-aminothiazole in CH₂Cl₂ leads to the heterobicyclic compounds [(triphos)(CO)₂Re{C=C(H)C(Ph)₂N(H)C(CH₂)₄N)}]OTf (**6**) and [(triphos)(CO)₂Re{C=C(H)C(Ph)₂N(H)CS(CH₂)₂N)}]OTf (**8**), respectively. Both complexes undergo regioselective deprotonation at the N–H heterocycle group by treatment with sodium methoxide in THF, giving the neutral species [(triphos)(CO)₂Re{C=C(H)C(Ph)₂NC(CH₂)₄N)}] (**7**) and [(triphos)(CO)₂Re{C=C(H)C(Ph)₂NCS(CH₂)₂N)}] (**9**), respectively. The X-ray structures of the new organorhenium species **4** and **7–9** have been determined, which have confirmed that the addition of the NH bond of the N,N-heterocycle occurs always across the C_β–C_γ double bond of the allenylidene chain.

Introduction

The development of highly efficient and selective synthetic methods of organic compounds is a crucial task for chemical research, due to the increasing market demand for fine chemicals. In this respect, the formation of carbon–carbon and carbon–heteroatom bonds, mediated by transition-metal complexes in stoichiometric and catalytic reactions, is important to bring about the synthesis of valuable products and intermediates for organic chemistry.¹ Relevant to this field are ruthenium unsaturated carbenes, Ru=C=C(_n)=CRR', particularly vinyl-

idenes (*n* = 0) and allenylidenes (*n* = 1), which in the past decade have led to the successful accomplishment of several stoichiometric and catalytic processes² characterized by high efficiency, high selectivity, and minimal environmental impact (atom economy processes). In the particular case of transition-metal allenylidenes, the high reactivity and the excellent adaptability in promoting C–C and C–X bond forming reactions has been related to the unique electronic properties of the tetratomic M=C=C=C array.^{2h,i} Indeed, theoretical calculations^{2h,3} and experimental² evidence have shown that the π-acceptor component of the metal–allenylidene bond is stronger than the σ-donor one and that the α- and γ-carbon atoms of the allenylidene chain are electrophilic centers, while

[†] Laboratorio di Chimica Nucleare ed Inorganica, Dipartimento di Chimica, Università di Ferrara.

[‡] Centro di Strutturistica Diffraattometrica, Dipartimento di Chimica, Università di Ferrara.

[§] ICCOM CNR.

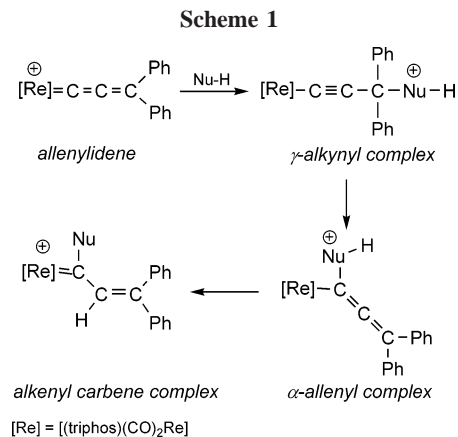
^{||} University of Cadiz.

(1) (a) Collman, J. P.; Hegedus, L. S.; Norton, J. R.; Finke, R. G. *Principles and Application of Organotransition Metal Chemistry*; University Science Books: Mill Valley, CA, 1987. (b) Brown, J. M.; Cooley, N. A. *Chem. Rev.* **1988**, *88*, 1031. (c) Brookhart, M.; Volpe, A. F., Jr.; Yoon, J. In *Comprehensive Organic Synthesis*; Trost, B. M., Fleming, I., Eds.; Pergamon Press: New York, 1991; Vol. 4. (d) Schmalz, H. G. *Angew. Chem., Int. Ed. Engl.* **1995**, *34*, 1833.

(2) (a) Esteruelas, M. A.; Gómez, A. V.; López, A. M.; Modrego, J.; Oñate, E. *Organometallics* **1997**, *16*, 5826. (b) Werner, H. *Chem. Commun.* **1997**, 903. (c) Bruce, M. I. *Chem. Rev.* **1998**, *98*, 2797. (d) Touchard, D.; Dixneuf, P. H. *Coord. Chem. Rev.* **1998**, *178–180*, 409. (e) Bruneau, C.; Dixneuf, P. H. *Acc. Chem. Res.* **1999**, *32*, 311. (f) Puerta, M. C.; Valerga, P. *Coord. Chem. Rev.* **1999**, *193–195*, 977. (g) Baya, M.; Crochet, P.; Esteruelas, M. A.; Gutiérrez-Puebla, E.; López, A. M.; Modrego, J.; Oñate, E.; Vela, N. *Organometallics* **2000**, *19*, 2585. (h) Cadierno, V.; Gamasa, M. P.; Gimeno, J. *Eur. J. Inorg. Chem.* **2001**, 571. (i) Bruneau, C. *Top. Organomet. Chem.* **2004**, *11*, 125.

the β -carbon atom is nucleophilic. Moreover, the reactivity of the MC_3 moiety may be further modulated by additional tunable factors, including the electronic nature of the metallic center and the ancillary ligands, the overall charge of the compound, and the steric and electronic properties of the C_γ substituents.^{4,5} During our ongoing research in this area, we have found that the highly stable rhenium(I) complex [(triphos)(CO)₂Re(OTf)] (triphos = MeC(CH₂PPh₂)₃; OTf = OSO₂CF₃) is a versatile precursor for the synthesis of a large variety of rhenium(I) complexes.^{6,7} This is related to the high lability of the triflate ligand, which is easily promoted in solution by a number of σ - and π -donor molecules, including unusual ligands such as white phosphorus,^{7a} hydrogen sulfide,^{7b} and tetraphosphorus trisulfide.^{7c}

Among the many organorhenium(I) derivatives stabilized by the [(triphos)(CO)₂Re]⁺ synthon, we described the first rhenium(I) allenylidenes, which were easily obtained by the Selegue protocol⁸ following triflate displacement by propargylic alcohols.^{9–11} The reactivity of these allenylidene compounds, particularly of the highly stable diphenyl derivative [(triphos)(CO)₂Re{C=C=CPh₂}]OTf (**1**), with nucleophilic reagents has been thoroughly investigated, with the aim of finding new synthetic protocols starting from basic hydrocarbon units.^{10,12} In summary, the diphenylallenylidene moiety in **1** does not add weak nucleophiles such as water and alcohols but readily reacts with a variety of ionic nucleophiles such as methoxide, hydroxide, hydride, and alkyl, leading to functionalized alkynyl compounds of the formula [(triphos)(CO)₂Re{C≡CC(R)(Ph)₂}] (R = OMe, OH, H, Me), via regioselective addition at the γ -carbon atom of the nucleophiles.^{10b} A variety of thiols,¹² amines,¹² and phosphines¹³ also add to the allenylidene ligand, affording the corresponding addition products. A mechanism encompassing the preliminary attack at C_γ to form γ -substituted alkynyl derivatives has been proposed and experimentally substantiated for the reaction with ammonia and secondary phosphines. The reaction usually proceeds with the C_γ to C_α nucleophile migration to yield α -allenyl species. These eventually may undergo X–H addition (X = N, P, S) across the C_α – C_β bond, resulting in the final alkenylcarbene derivatives. Scheme 1 highlights the proposed mechanism accounting for the addition of simple nucleophiles to **1**. Remarkably, when primary amines and phosphines are used, azonia- and phos-



phoniabutadienyl derivatives are obtained in preference to the isomeric amino- and phosphinocarbenes.^{12,13}

To further exploit the potential reactivity of the rhenium allenylidene chain, we decided to investigate the chemistry of **1** with polyfunctionalized organic molecules containing at least two nucleophilic heteroatoms and one electrophilic hydrogen atom. Several organic substrates bearing two nucleophilic ends and one electrophilic center may be used to verify this hypothesis. These include both five- and six-membered molecules bearing nitrogen and/or sulfur atoms in the heterocyclic ring bearing pendant heteroatomic substituents (amino, –NH₂, or thiol, –SH) or their combinations. Following our preliminary report illustrating the reaction of **1** with pyrazole,¹⁴ herein we extend this chemistry to other nitrogen heterocycles, while in a further publication the reactivity of **1** with heterocyclic thioles will be highlighted. Examples of this chemical reactivity have been seldom considered, and to the best of our knowledge, they are limited only to the ruthenium(II) diphenylallenylidene complex [Cp(CO)(PPrⁱ)₃Ru{C=C=CPh₂}]BF₄.^{15–17}

Results and Discussion

General Considerations. 1,2,3-Diheterocyclization readily occurs when the allenylidene ligand in **1** is treated with a variety of N,N-heterocycles such as pyrazole, 1H-benzotriazole, 2-aminopyridine, and 2-aminothiazole. Organometallic heteropolycyclic compounds built on allenylidenes and containing heterocycles derived from 1H-benzotriazole and 2-aminothiazole are so far unknown, while related organoruthenium species derived from 2-aminopyridine and pyrazole have been described by Esteruelas and co-workers.¹⁵ All of the new organorhenium(I) compounds have been characterized by elemental analysis and conventional spectroscopic measurements and, for some representative species, by X-ray crystallography (see the specific section below). Selected IR and NMR spectral data are given in Table 1 for all the new complexes. As the structure of the cationic rhenium(I) synthon [(triphos)Re(CO)₂]⁺, formed by the tripodal polyphosphine and the two carbonyl ligands, remains unchanged in all the organorhenium complexes described in this article, a few common spectroscopic features may be sum-

(3) For a theoretical analysis of the allenylidene reactivity, see: (a) Re, N.; Sgamellotti, A.; Floriani, C. *Organometallics* **2000**, *19*, 1115. (b) Marrone, A.; Re, N. *Organometallics* **2002**, *21*, 3562. (c) Marrone, A.; Coletti, C.; Re, N. *Organometallics* **2004**, *23*, 4952.

(4) Mantovani, N.; Marvelli, L.; Rossi, R.; Bianchini, C.; De los Rios, I.; Romerosa, A.; Peruzzini, M. *Dalton Trans.* **2001**, 2353.

(5) Bruce, M. I. *Coord. Chem. Rev.* **2004**, *248*, 1603.

(6) Bergamini, P.; Fabrizi De Biani, F.; Marvelli, L.; Mascellani, N.; Peruzzini, M.; Rossi, R.; Zanella, P. *New J. Chem.* **1999**, 207.

(7) (a) Peruzzini, M.; Marvelli, L.; Romerosa, A.; Rossi, R.; Vizza, F.; Zanobini, F. *Eur. J. Inorg. Chem.* **1999**, 931. (b) Peruzzini, M.; De los Rios, I.; Romerosa, A. *Prog. Inorg. Chem.* **2001**, *49*, 163. (c) Guidoboni, E.; De los Rios, I.; Ienco, A.; Marvelli, L.; Mealli, C.; Romerosa, A.; Rossi, R.; Peruzzini, M. *Inorg. Chem.* **2002**, *41*, 659.

(8) Selegue, J. P. *Organometallics* **1982**, *1*, 217.

(9) Bianchini, C.; Mantovani, N.; Marchi, A.; Marvelli, L.; Masi, D.; Peruzzini, M.; Rossi, R.; Romerosa, A. *Organometallics* **1999**, *18*, 4501.

(10) (a) Bianchini, C.; Mantovani, N.; Marvelli, L.; Peruzzini, M.; Romerosa, A.; Rossi, R. *J. Organomet. Chem.* **2001**, *617–618*, 233. (b) Mantovani, N.; Marvelli, L.; Rossi, R.; Bianchini, C.; De los Rios, I.; Romerosa, A.; Peruzzini, M. *J. Chem. Soc., Dalton Trans.* **2001**, 2353.

(11) (a) Bianchini, C.; Marchi, A.; Marvelli, L.; Masi, D.; Peruzzini, M.; Rossi, R. *Eur. J. Inorg. Chem.* **1998**, 211. (b) Peruzzini, M.; Akbayeva, D.; Bianchini, C.; De los Rios, I.; Ienco, A.; Mantovani, N.; Marvelli, L.; Rossi, R. *Inorg. Chim. Acta* **2002**, *339*, 202.

(12) Mantovani, N.; Marvelli, L.; Rossi, R.; Bertolasi, V.; Bianchini, C.; De los Rios, I.; Peruzzini, M. *Organometallics* **2002**, *21*, 2382.

(13) Peruzzini, M.; Barbaro, P.; Bertolasi, V.; Bianchini, C.; De los Rios, I.; Mantovani, N.; Marvelli, L.; Rossi, R. *Dalton Trans.* **2003**, 4121.

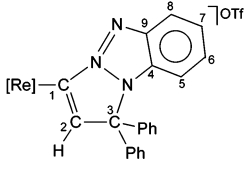
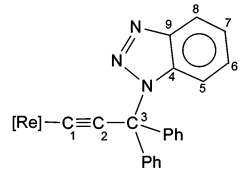
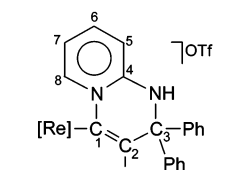
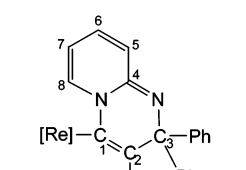
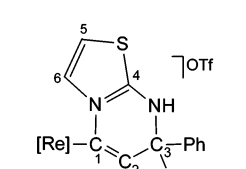
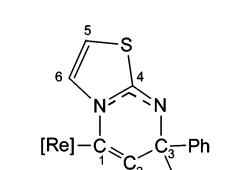
(14) Bertolasi, V.; Mantovani, N.; Marvelli, L.; Rossi, R.; Bianchini, C.; De los Rios, I.; Peruzzini, M.; Akbayeva, D. N. *Inorg. Chim. Acta* **2003**, *344*, 207.

(15) Esteruelas, M. A.; Gómez, A. V.; López, A. M.; Oñate, E. *Organometallics* **1998**, *17*, 3567.

(16) Bernad, D. J.; Esteruelas, M. A.; López, A. M.; Oliván, M.; Oñate, E.; Puerta, M. C.; Valerga, P. *Organometallics* **2000**, *19*, 4327.

(17) Esteruelas, M. A.; López, A. M. In *Recent Advances in Hydride Chemistry*; Peruzzini, M., Poli, R., Eds.; Elsevier: Amsterdam, 2001; Chapter 7, pp 212–213.

Table 1. Selected ^1H , $^{13}\text{C}\{^1\text{H}\}$, and $^{31}\text{P}\{^1\text{H}\}$ NMR Spectral Data and IR Absorptions for the Rhenium Complexes

Complexes	^1H δ (ppm), J (Hz)	$^{13}\text{C}\{^1\text{H}\}^f$ δ (ppm), J (Hz)	$^{31}\text{P}\{^1\text{H}\}^g$ δ (ppm), J (Hz)	
			IR (KBr, cm^{-1})	
 4 ^a	1.63 (q, J_{HP} 2.7, 3H, CH_3 triphos) 2.65 (d, J_{HP} 8.7, 2H, CH_2 Pax triphos) 2.40-2.85 (br m, 4H, CH_2 Peq triphos) ^c $\text{CH}_{(\text{C}2)} + \text{CH}_{(\text{C}5, \text{C}6, \text{C}7, \text{C}8)}$	197.7 (dm, J_{CP} 32, CO) 147.7 ^c (dt, J_{CPtrans} 34, J_{CPcis} 8.7, C1) 119.1 ^c (s, C2) 82.9 ^c (s, C3) ^c $\text{CH}_{(\text{C}5, \text{C}6, \text{C}7, \text{C}8)}$ ^c C(C4, C9)	δ_{A} -8.16 J_{AM} 19.2 δ_{M} -16.10 <hr/> v(CO) 1950, 1887 v(C=C), (C=N) 1610, 1581 v(OTf) 1275	
 5 ^a	1.52 (br s, 3H, CH_3 triphos) 2.10-2.80 (br m, 6H, CH_2 triphos) ^c $\text{CH}_{(\text{C}5, \text{C}6, \text{C}7, \text{C}8)}$	198.0 (m, CO) 119.2 (s, C2) 116.1 (s, C1) ^c C5, C6, C7, C8 66.2 (s, C3)	δ_{A} -7.82 J_{AM} 17.9 δ_{M} -19.68 <hr/> v(C≡C) 2091 v(CO) 1950, 1885 v(C=C), (C=N) br 1580	
 6 ^a	1.65 (q, J_{HP} 2.0, 3H, CH_3 triphos) 2.58 (d, J_{HP} 8.1, 2H, CH_2 -P _{ax} triphos) 2.78-2.83 (br m, 4H, CH_2 -P _{eq} triphos) 5.63 ^d (t, J_{HH} 6.9, 1H, $\text{CH}_{(\text{C}7)}$) 6.14 ^d (br s, 1H, $\text{CH}_{(\text{C}2)}$) 7.03 ^d (t, J_{HH} 6.9, 1H, $\text{CH}_{(\text{C}6)}$) 7.25 ^d (t, J_{HH} 6.9, 1H, $\text{CH}_{(\text{C}5)}$) 8.29 ^d (d, J_{HH} 6.7, 1H, $\text{CH}_{(\text{C}8)}$) 9.16 (br s, 1H, ω_2 6 Hz, NH)	200.0 (dm, J_{CPtrans} 33.2, CO) 145.8 ^c (s, C4) 143.9 ^c (s, C8) 139.8 ^c (s, C5) 139.6 ^c (dt, J_{CPtrans} 44.0, J_{CPcis} 2.0, C1) 137.8 ^c (s, C7) 115.4 ^c (s, C6) 111.0 ^c (s, C2) 62.2 ^c (s, C3)	δ_{A} -13.49 J_{AM} 16.9 δ_{M} -14.33 <hr/> v(NH) 3320 v(CO) 1946, 1880 v(C=C), (C=N) 1644, 1580 v(OTf) 1283	
 7 ^b	1.58 (br s, 3H, CH_3 triphos) 2.10-2.80 (br m 6H, CH_2 triphos) 4.80 (dd, J_{HH} 1.8, J_{HH} 6.1, 1H, $\text{CH}_{(\text{C}6)}$) 5.61 (d, J_{HH} 1.8, 1H, $\text{CH}_{(\text{C}5)}$) 6.31 (dd, J_{HH} 6.7, J_{HH} 6.1, 1H, $\text{CH}_{(\text{C}7)}$) 6.66 (d, J_{HP} 9.1, 1H, $\text{CH}_{(\text{C}2)}$) 7.66 (d, J_{HH} 6.7, 1H, $\text{CH}_{(\text{C}8)}$)	200.1 (dm, J_{CPtrans} 42.6, CO) 151.0 (d, J_{CPtrans} 14.2, C1) 141.7; 140.5; 139.6; 131.7; 121.4 (all s, C4, C5, C6, C7, C8) 100.7 (s, C2) 64.5 (s, C3)	δ_{A} -12.12 J_{AM} 14.8 δ_{M} -15.68 <hr/> v(CO) 1941, 1870 v(C=C), (C=N) 1634, 1571	
 8 ^a	1.61 (q, J_{HP} 2.4, 3H, CH_3 triphos) 2.51-2.76 (br m, 2H, CH_2 -P _{ax} triphos) 2.62 (d, J_{HP} 8.7, 4H, CH_2 -P _{eq} triphos) 5.61 ^d (d, J_{HH} 4.6, 1H, $\text{CH}_{(\text{C}5)}$) 5.80 ^d (d, J_{HP} 2.1, 1H, $\text{CH}_{(\text{C}2)}$) 7.30 ^d (d, J_{HH} 4.6, 1H, $\text{CH}_{(\text{C}6)}$)	200.2 (m, CO) 161.1 ^c (s, C4) 145.5 ^c (s, C5) 139.6 ^c (dt, J_{CPtrans} 43.8, J_{CPcis} 2.1, C1) 135.0 ^c (s, C6) 101.1 ^c (s, C2) 62.8 ^c (s, C3)	δ_{A} -13.71 J_{AM} 17.5 δ_{M} -14.88 <hr/> v(NH) 3319 v(CO) 1941, 1875 v(C=C), (C=N) 1599, 1580 v(OTf) 1281	
 9 ^b	1.53 (br s, 3H, CH_3 triphos) 2.30-2.60 (br m, 6H, CH_2 triphos) 4.77 (d, J_{HH} 4.9, 1H, $\text{CH}_{(\text{C}5)}$) 5.30 (d, J_{HP} 2.4, 1H, $\text{CH}_{(\text{C}2)}$) 6.74 (d, J_{HH} 4.9, 1H, $\text{CH}_{(\text{C}6)}$)	201.5 (m, CO) 158.7 (s, C4) 151.4 (s, C6) 140.9 (d, J_{CPtrans} 42.7, C1) 134.8 (s, C5) 93.7 (s, C2) 68.7 (s, C3)	δ_{A} -12.37 J_{AM} 16.4 δ_{M} -15.47 <hr/> v(CO) 1944, 1867 v(C=C), (C=N) 1604, 1574	

^a [Re] indicates the [(triphos)Re(CO)₂]⁺ moiety. The NMR spectra were recorded in CD₂Cl₂, unless otherwise stated, at room temperature using a Varian VXR300 instrument. Key: s, singlet; d, doublet; t, triplet; q, quartet; m, multiplet; br, broad. ^b Recorded in CDCl₃. ^c Assigned by DEPT-135 experiment. ^d Assigned by $^1\text{H}, ^1\text{H}$ -2D COSY NMR experiment. ^e CH(ring) not observed, likely masked by the aromatic resonances. ^f The $^{13}\text{C}\{^1\text{H}\}$ NMR signals of the triphos ligand are given in the Experimental Section. ^g All $^{31}\text{P}\{^1\text{H}\}$ NMR spectra exhibit an AM₂ splitting pattern.

marized as follows: (i) the $^{31}\text{P}\{^1\text{H}\}$ NMR spectrum of each complex exhibits an AM₂ spin system with a triplet assigned to the phosphorus atom trans to the organorhenium ligand, P_A ($-8.16 \leq \delta \leq -13.71$ ppm), and a doublet due to the two

chemically equivalent phosphorus atoms lying trans to CO, P_M ($-14.33 \leq \delta \leq -16.10$ ppm); (ii) the $^{13}\text{C}\{^1\text{H}\}$ NMR spectra show an AMM'XX' multiplet near 200 ppm due to the two magnetically inequivalent carbonyl carbon atoms; ^{4,6,7,9-12} (iii)

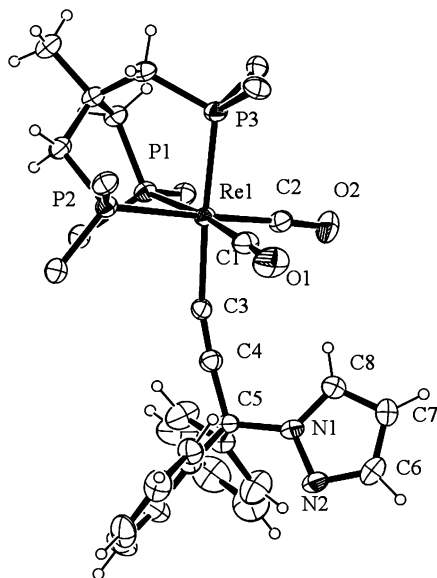
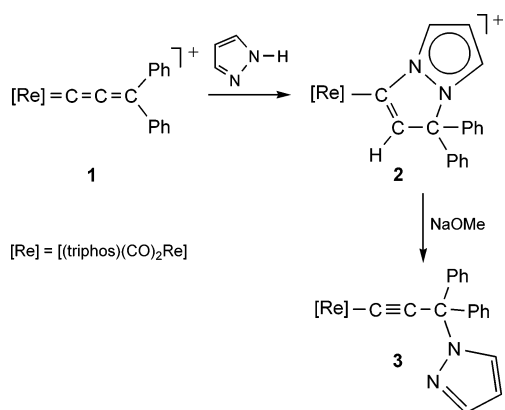


Figure 1. ORTEP view of the complex **3**. The ellipsoids are drawn at the 30% probability level. Only the ipso carbons of the phenyl rings of the triphos ligand are shown for the sake of clarity.

Scheme 2



the IR spectra display two strong IR bands at ca. 1950 and 1880 cm^{-1} for the asymmetric and antisymmetric stretching of the carbonyl ligands.^{4,6,7,9–12}

Reaction of 1 with 1*H*-Benzotriazole. We have shown previously that **1** reacts with pyrazole to afford the heterobicyclic product $[(\text{triphos})(\text{CO})_2\text{Re}\{\text{C}=\text{C}(\text{H})\text{C}(\text{Ph})_2\text{N}(\text{CH}_3)_3\text{N}\}]\text{OTf}$ (**2**) via 1,2,3-diheterocyclization at the allenylidene moiety.¹⁴ Deprotonation of **2** with NaOMe yields the pyrazolylalkynyl species $[(\text{triphos})(\text{CO})_2\text{Re}\{\text{C}\equiv\text{C}(\text{Ph})_2\text{N}(\text{CH}_3)_3\text{N}\}]$ (**3**) via reversible back-opening of the N–C $_{\alpha}$ bond of the heterocyclic derivative **2** (Scheme 2). As we have been able to grow crystals of **3** suitable for an X-ray diffraction study, we present here details of this crystallographic analysis. The crystal structure of complex **3** is shown in Figure 1, while selected bond distances and angles are reported in Tables 2 and 3.

To verify whether other nitrogen heterocycles are endowed with similar reactivity toward **1**, we have treated the rhenium allenylidene complex with five- and six-membered N-heterocycles, including pyrrole, imidazole, pyridine, quinoline, and 1*H*-benzotriazole. While pyridine, quinoline, pyrrole, and imidazole do not react with **1** even under harsh reaction conditions (prolonged reflux of **1** dissolved in the neat heterocycle or in a concentrated THF solution of the heterocycle), the reaction with 1*H*-benzotriazole, which shares with pyrazole the structural

Table 2. Selected Bond Distances (Å)

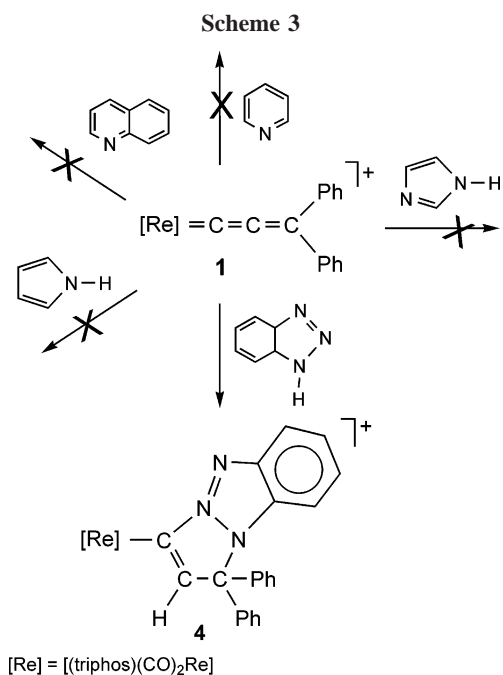
	3	4	7	8	9
Re1–P1	2.460(1)	2.473(1)	2.504(2)	2.509(2)	2.493(1)
Re1–P2	2.469(1)	2.493(1)	2.501(1)	2.488(2)	2.507(1)
Re1–P3	2.394(2)	2.446(1)	2.428(2)	2.430(2)	2.430(1)
Re1–C1	1.918(6)	1.915(2)	1.920(9)	1.926(8)	1.918(6)
Re1–C2	1.913(6)	1.928(2)	1.904(7)	1.917(7)	1.902(4)
Re1–C3	2.118(5)	2.168(3)	2.239(6)	2.235(7)	2.223(4)
C1–O1	1.151(8)	1.158(8)	1.145(8)	1.141(11)	1.149(8)
C2–O2	1.158(8)	1.136(8)	1.149(9)	1.166(10)	1.165(6)
C3–C4	1.203(8)	1.344(4)	1.325(12)	1.323(10)	1.349(7)
C4–C5	1.471(8)	1.524(4)	1.522(10)	1.526(11)	1.520(6)
N1–C5	1.507(7)	1.477(3)	1.477(10)	1.477(10)	1.478(6)
N1–C6		1.363(3)	1.279(13)	1.334(10)	1.276(7)
N1–N2	1.349(6)	1.351(3)			
N1–C8	1.328(8)				
N2–N3		1.296(2)			
N2–C3		1.455(3)	1.452(7)	1.484(9)	1.439(5)
N2–C6	1.330(8)		1.431(10)	1.331(11)	1.399(5)
N2–C7			1.379(13)	1.387(9)	1.401(8)
N3–C11		1.374(4)			
C6–C7	1.366(10)				
C6–C10			1.423(12)		
C6–C11		1.411(4)			
C7–C8	1.364(9)		1.348(11)	1.330(12)	1.332(6)
C8–C9			1.393(16)		
C9–C10			1.365(19)		
S1–C6				1.723(7)	1.764(5)
S1–C8				1.726(10)	1.734(6)

Table 3. Selected Bond Angles (deg)

	3	4	7	8	9
P1–Re1–P2	81.46(5)	84.48(2)	82.28(6)	83.61(5)	83.17(4)
P1–Re1–P3	86.80(5)	88.10(2)	85.05(6)	86.49(6)	85.34(4)
P1–Re1–C1	173.9(2)	174.0(1)	174.8(2)	173.9(2)	176.3(2)
P1–Re1–C2	97.2(2)	90.4(1)	99.4(3)	98.5(2)	96.9(2)
P1–Re1–C3	92.7(2)	93.6(1)	101.0(2)	95.1(2)	101.4(1)
P2–Re1–P3	86.45(5)	83.46(2)	88.97(6)	83.89(6)	88.73(3)
P2–Re1–C1	95.1(1)	100.4(1)	93.3(2)	92.3(2)	94.5(1)
P2–Re1–C2	177.7(2)	174.1(1)	178.3(3)	174.9(2)	177.2(2)
P2–Re1–C3	98.3(1)	93.5(1)	89.0(2)	98.1(2)	88.5(1)
P3–Re1–C1	98.0(2)	95.8(1)	92.2(2)	97.6(2)	91.8(1)
P3–Re1–C2	91.6(2)	93.5(1)	91.0(2)	91.6(2)	94.1(2)
P3–Re1–C3	175.1(2)	176.3(1)	173.3(2)	177.6(2)	172.4(1)
C1–Re1–C2	86.4(2)	84.9(1)	85.0(3)	86.0(3)	85.6(2)
C1–Re1–C3	82.8(2)	82.8(1)	81.6(3)	81.0(3)	81.4(2)
C2–Re1–C3	83.6(2)	89.7(1)	90.8(3)	86.4(3)	88.7(2)
Re1–C3–C4	167.8(5)	136.5(2)	121.7(5)	126.2(5)	122.9(3)
Re1–C3–N2		120.3(2)	126.0(4)	120.3(5)	125.3(2)
N2–C3–C4		102.0(2)	112.2(5)	112.0(6)	111.6(3)
C3–C4–C5	174.8(6)	116.3(2)	124.5(6)	126.3(6)	124.4(4)
C4–C5–N1	107.1(4)	97.9(2)	109.7(5)	106.1(6)	110.2(3)
C5–N1–C6		142.1(2)	116.6(6)	118.1(6)	113.5(4)
C5–N1–N2	121.4(4)	110.4(2)			
N2–N1–C6		107.3(2)			
N2–N1–C8	111.0(5)				
N1–N2–N3		113.8(2)			
C3–N2–C6			118.5(5)	121.1(6)	118.0(3)
N2–N3–C11		104.5(2)			
N1–C6–N2			123.2(8)	122.1(6)	127.4(4)
N1–C6–C11		104.1(2)			
N3–C11–C6		110.1(2)			

(H)N–N motif, takes place also at room temperature in dichloromethane.

When the reaction of **1** and 1*H*-benzotriazole is carried out in dichloromethane, orange microcrystals of $[(\text{triphos})(\text{CO})_2\text{Re}\{\text{C}=\text{C}(\text{H})\text{C}(\text{Ph})_2\text{N}(\text{C}_6\text{H}_4)\text{N}=\text{N}\}]\text{OTf}$ (**4-OTf**) are obtained after working up the solution (Scheme 3). The elemental analysis confirms the incorporation of the intact benzotriazole molecule in the product, while NMR spectroscopy clearly indicates that a structural motif similar to that of **2** as been assembled onto



the rhenium allenylidene moiety. Particularly informative are the three resonances at 147.7, 119.1, and 82.9 ppm in the ¹³C-¹H NMR spectrum assigned to the three carbon atoms of the allenylidene unit incorporated in the metal-supported 1,1-diphenyl-1*H*-3a,8-diaza-8a-azoniacyclopenta[*a*]indene skeleton of the heterotricyclic ligand. In agreement with the presence of both C=C and C=N bonds in **4**, the IR spectrum shows absorptions at 1610 and 1581 cm⁻¹. Finally, a band at 1275 cm⁻¹ is consistent with the presence of a triflate anion not coordinated to the metal center.¹⁸ Metathesis with NaBPh₄ in ethanol yields the tetraphenylborate salt of **4**, which shares with the triflate salt all of the main chemico-physical properties ($\nu_{\text{BC}} = 611 \text{ cm}^{-1}$).

Remarkably, the lack of reactivity of **1** with all of the tested *N*-heterocycles, except with 1*H*-benzotriazole, is mechanistically relevant, pointing out that an assembly of two nucleophilic heteroatoms and one electrophilic hydrogen atom are mandatory to accomplish the heterocyclization at the ReC₃ moiety.¹⁹

An inspection of only the spectroscopic data does not allow us to establish the exact structure of complex **4** in solution, since two orientations are possible for the addition of the NH group of benzotriazole to the allenylidene ligand, (i.e. N → C_α (**4a**) or N → C_γ (**4b**), together with H → C_β; Scheme 4). Although on the basis of the general mechanism highlighted in Scheme 1 the pathway involving nitrogen attack at C_γ seems to be more probable, only the X-ray crystal structure allowed us to definitely identify the reaction product as **4b**. The crystal structure of the rhenium cation of **4-BPh₄** is shown in Figure 2, while selected bond distances and angles are provided in Tables 2 and 3.

Remarkably, the heterocyclization reaction is totally regioselective, as no trace of the alternative isomer **4a** is detected by monitoring the reaction of **1** with benzotriazole by ¹H NMR in CD₂Cl₂. The same experiment, carried out by progressively increasing the temperature from -78 to 25 °C, indicates that the heterocyclization starts at ca. 10 °C and progresses until complete conversion to the final heterocyclized product **4b** without any detectable intermediate species.

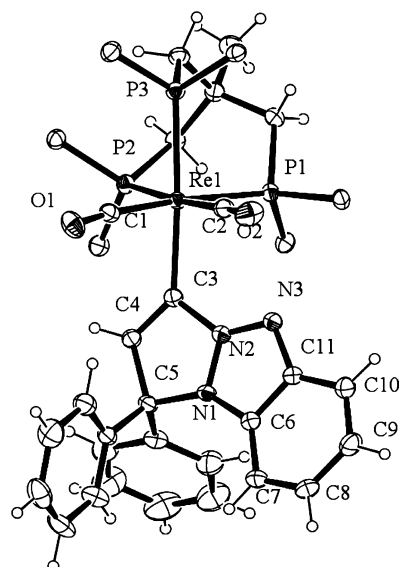
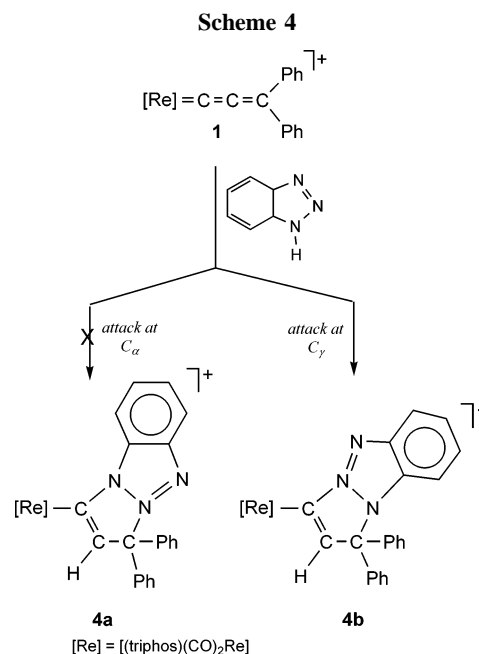


Figure 2. ORTEP view of the complex cation of **4**. The ellipsoids are drawn at the 30% probability level. Only the ipso carbons of the phenyl rings of the triphos ligand are shown for the sake of clarity.



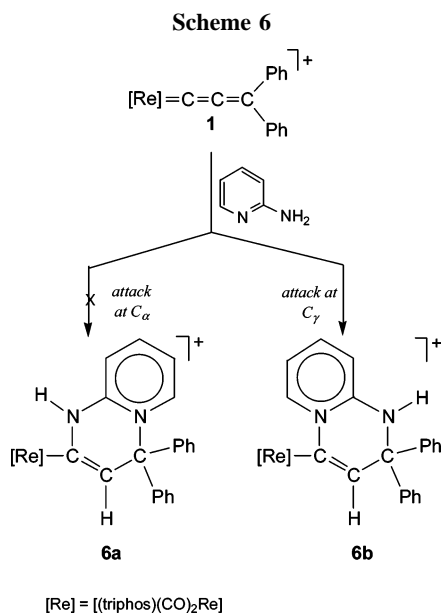
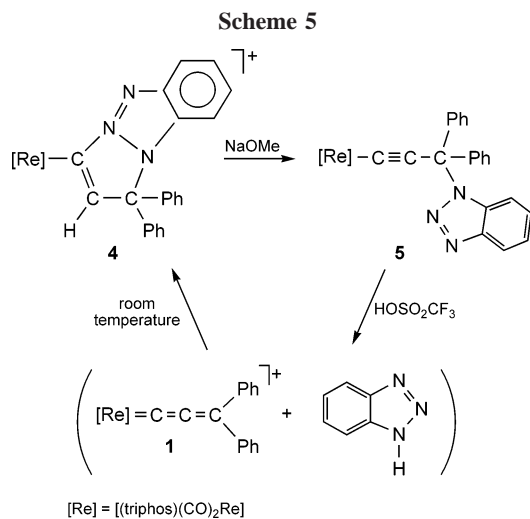
Similarly to complex **2**, also **4** selectively deprotonates when treated with sodium methoxide in tetrahydrofuran at room temperature, leading to the functionalized alkynyl derivative [(triphos)(CO)₂Re{C≡CC(Ph)₂(NC₆H₄N=N)}] (**5**). This latter species may be converted back to **4** with the same pathway found for **2** and **3** by following the route summarized in Scheme 5.

In keeping with the presence of a σ -alkynyl ligand, the IR spectrum of **5** exhibits a strong and sharp $\nu_{\text{C}\equiv\text{C}}$ absorption at 2091 cm⁻¹, while in the ¹³C-¹H NMR spectrum C_α, C_β, and C_γ are observed at 116.1, 119.2, and 66.2 ppm, respectively.

Reaction of 1 with 2-Aminopyridine. Treatment of a dichloromethane solution of **1** with 5 equiv of 2-aminopyridine leads, after the usual workup, to the new complex [(triphos)(CO)₂Re{C=C(H)C(Ph)₂N(H)C(CH₂)₄N}]OTf (**6**), which has been isolated as a yellow crystalline product in excellent yield.

(18) Lawrance, G. G. A. *Chem. Rev.* **1986**, *86*, 17.

(19) 1*H*-Benzotriazole ($pK_a = 8.50$) is a weaker acid than imidazole ($pK_a = 6.95$). See: Slater, A.; McCormack, A.; Avdeef, A.; Comer, J. E. A. *J. Pharm. Sci.* **1994**, *83*, 1280.



The presence in **6** of a rhenaheterobicyclic system, derived from the condensation of the metallacumulene moiety with the aminopyridine, is confirmed by the NMR analysis, which strictly parallels those discussed above for **2** and **4**.¹⁴ Particularly informative is the $^{13}\text{C}\{^1\text{H}\}$ NMR spectrum, with three resonances due to the heterocyclized C_α , C_β , and C_γ carbon atoms at 139.6, 111.0, and 62.2 ppm, respectively. In the ^1H NMR spectrum, the vinylic proton appears as a slightly broadened singlet at 6.14 ppm, correlating to the C_β carbon (2D- ^1H , ^{13}C -HMQC NMR). The presence of the NH proton is confirmed by a featureless hump at 9.16 ppm and by an IR absorption in the region expected for N–H stretching (ν_{NH} 3320 cm^{-1}).

Similarly to **4**, even if two orientations are possible (**6a** and **6b** in Scheme 6) for the addition of the 2-aminopyridine to the allenylidene, the reaction takes place with complete regioselectivity, as shown by the observation of a single AM_2 ^{31}P NMR pattern. Although the NMR data alone cannot discriminate between the two possible adducts, the X-ray analysis of the N-deprotonated derivative **7** (see below) unequivocally establishes that the pyridinium complex **6** is formed via regioselective NH_2 attack of the aminopyridine to C_γ .

The deprotonation of the NH amine group, rather than of the vinylic CH, occurs by reacting **6** with sodium methoxide in THF. The reaction yields the pyrido[1,2-*a*]pyrimidinyl derivative **7** (Scheme 7), which has been characterized by X-ray methods

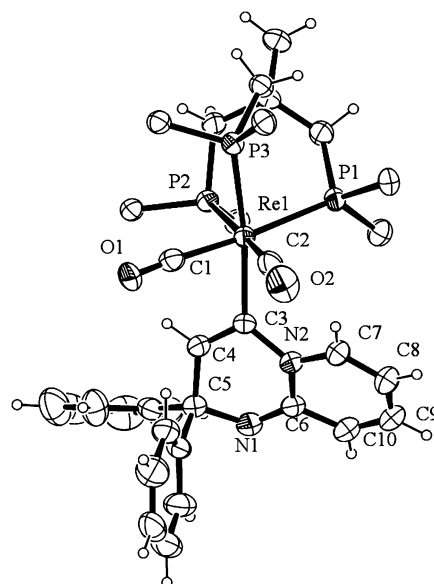
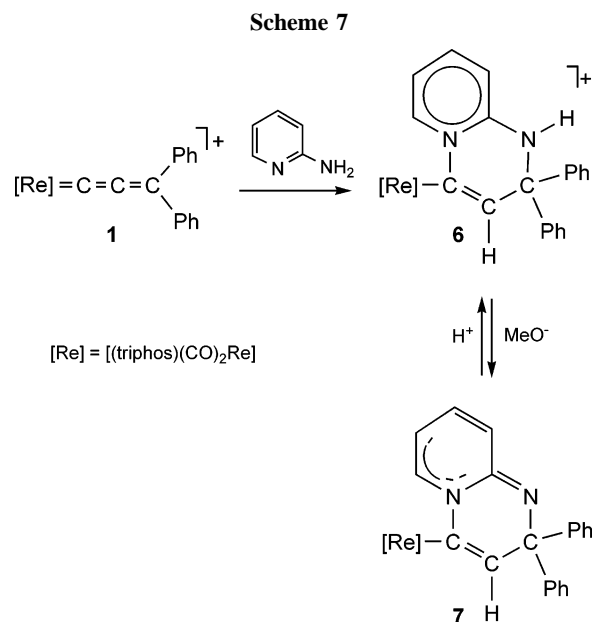


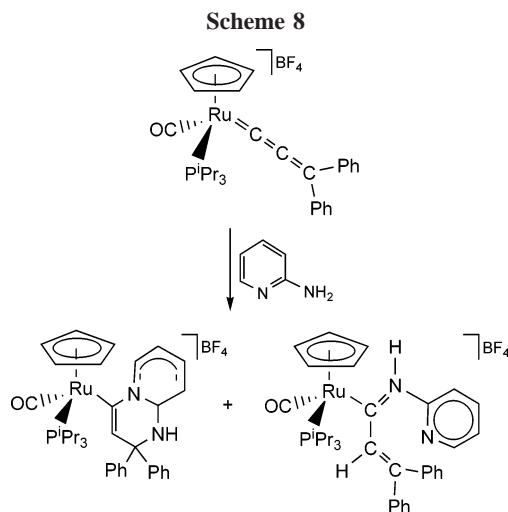
Figure 3. ORTEP view of the complex **7**. The ellipsoids are drawn at the 30% probability level. Only the ipso carbons of the phenyl rings of the triphos ligand are shown for the sake of clarity.



(see Figure 3 and Tables 2 and 3). The relevant spectroscopic data are listed in Table 1. The formation of **7** is completely reversible, and addition of triflic acid to **7** in dichloromethane immediately regenerates **6**.

The outcome of the reaction between **1** and 2-aminopyridine does not depend on the temperature, and the process remains strictly regioselective, irrespective of the reaction conditions. This behavior markedly contrasts with that reported by Esteruelas and co-workers for the corresponding reaction of $[\text{Cp}(\text{CO})(\text{PPr}^t_3)\text{Ru}\{\text{C}=\text{C}=\text{CPh}_2\}]\text{BF}_4$ with 2-aminopyridine. In that case, a temperature-dependent mixture of the pyridinium complex $[\text{Cp}(\text{CO})(\text{PPr}^t_3)\text{Ru}\{2,2\text{-diphenyl-2H-pyridinium}[1,2\text{-}a]\text{pyrimidin-4-yl}\}]\text{BF}_4$ and its azoniabutadienyl isomer $[\text{Cp}(\text{CO})(\text{PPr}^t_3)\text{Ru}\{\text{C}(\text{CH}=\text{CPh}_2)=\text{NH}(o\text{-pyridinyl})\}]\text{BF}_4$ was observed and a mechanistic interpretation of the reaction via a temperature-dependent amino–imino tautomeric equilibrium was provided (Scheme 8).^{16,17}

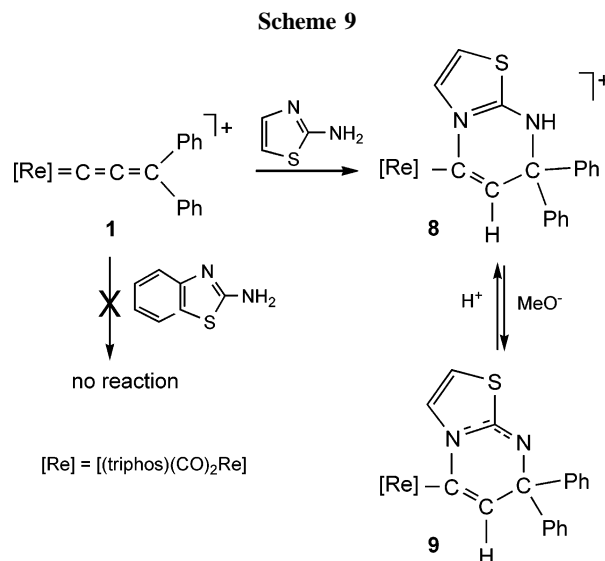
Reaction of 1 with 2-Aminothiazole and Related Molecules. The 1,2,3-diheterocyclization of the rhenium allenylidene



moiety takes place at room temperature when **1** is reacted with 1 equiv of 2-aminothiazole in dichloromethane. [(triphos)-(CO)₂Re{C=C(H)C(Ph)₂N(H)CS(CH₂)₂N}]OTf (**8**) is obtained in good yield after the usual workup. The tetraphenylborate salt of **8** was isolated from a EtOH solution after metathetical reaction with an excess of NaBPh₄. As for the other heterocyclized adducts described in this article, also the reaction with 2-aminothiazole exhibits a complete regioselectivity, as confirmed by the ³¹P{¹H} NMR spectrum, which shows only a single AM₂ pattern. The most interesting feature in the IR spectrum of **8** is the presence of ν(C=C) and ν(C=N) absorptions at 1599 and 1580 cm⁻¹, respectively, which are indicative of an extensive electronic delocalization along the N–C–N moiety of the heterocyclic ligand.²⁰ In the ¹H NMR spectrum, the resonance of the vinylic proton is a doublet at 5.80 ppm (*J*_{HP} = 2.1 Hz), whereas the two thiazolic hydrogens appear as doublets at 5.61 and 7.30 ppm (*J*_{HH} = 4.6 Hz). In the ¹³C{¹H} NMR spectrum, the C_α, C_β, and C_γ resonances fall in the expected regions (δ 139.6, 101.1, and 62.8, respectively). The other NMR signals and IR absorptions are provided in Table 1.

Similarly to **6**, the exocyclic nitrogen atom of **8** easily undergoes deprotonation when treated with NaOMe in THF to give the neutral thiazol-2-ylidene derivative **9** (Scheme 9).

The deprotonation is completely reversible, the resonances of **8** being fully restored on addition of HOTf to a dichloromethane solution of **9** (³¹P{¹H} NMR). The NMR data for **9** are consistent with the proposed formulation. The minor aromaticity of the thiazole protons accounts for their high-field shifting in the ¹H NMR spectrum (see Table 1). This observation is in agreement with the results of the crystal structure analysis (see below) of the two related species **8** and **9**, which are discussed in the crystallographic section below (see Figure 4 and Tables 2 and 3). These structural determinations remove any ambiguity in assigning the identity of the product of the addition of 2-aminothiazole to the Re=C=C=C moiety, ruling out three of the four possible different isomers (Chart 1). In fact, the molecular structure of **8** shows that the exocyclic nitrogen atom of the thiazol-2-ylamino substituent is bonded to the C_γ carbon atom and that the endocyclic nitrogen atom, rather than the sulfur atom, is linked to the C_α-allenylidene position (I). As a result, an unprecedented thiazol-2-ylamino



bicycle is built onto the organometallic platform formed by the rhenium cumulene precursor.

Under identical reaction conditions, **1** does not react with 2-aminobenzothiazole (Scheme 9). Apart from the fact that the steric hindrance of this heterocycle is higher than that of 2-aminothiazole, there is no obvious rationale for this behavior.

As a final comment on the reactivity of the rhenium allenylidene **1** toward dipolar heterocycles, it is worth mentioning that in 1988 we reported on the thioureido rhenium(I) dicarbonyl derivative [Re(PPh₃)₂(CO)₂{*N,S*-SC(=NPh)N(Me)(CSCH=CHN)}] (**11**), obtained by formal insertion of the heterocumulene PhN=C=S ligand into the Re–N bond of the *N*-methylaminothiazolate complex [(PPh₃)₂(CO)₂Re{*N,N'*-MeN(CSCH=CHN)}] (**10**) (Scheme 10).²⁰ This reactivity points out that the tendency of the rhenium allenylidene moiety in **1** to heterocyclize with the pseudoallyl functionality (N=C=N) of the 2-aminothiazole is also observed, mutatis mutandis, when the rhenium pseudoallyl moiety reacts with an heterocumulene ligand such as phenylisothiocyanate.

Crystallographic Studies. In addition to the four organorhenium compounds **4** and **7–9** resulting from the heterocyclization of 1*H*-benzotriazole, 2-aminopyridine, and 2-aminothiazole on the rhenium allenylidene moiety of **1**, we report in this section also on the molecular structure of the pyrazolyl alkynyl derivative **3**, which forms upon protonolysis of the pyrazole adduct **2** (see above, Scheme 2). Crystals of **3** suitable for a X-ray diffraction study were indeed obtained by slow crystallization from a dilute solution of **3** in CH₂Cl₂/petroleum ether (1:1).

In all the compounds **3**, **4**, and **7–9** (see Figures 1–5 above), the rhenium atom is octahedrally coordinated by a *fac*-triphos ligand, by two *cis* terminal carbonyls, and by a carbon atom of the corresponding organic ligand. The Re1–C3 bond distance in **3** (2.118(5) Å) is shorter than that reported for the 1,1-diphenyl-1*H*-pyrazolo[1,2-*a*]pyrazol-4-ylum complex **2** (2.171(4) Å), reflecting the different hybridization (sp vs sp²) of the C3 carbon, while the pyrazolic ring displays a similar π-delocalization.¹³ This trend is also observed for the Re1–P3 distances (2.442(1) Å in **2** and 2.394(2) Å in **3**). In both compounds these bonds, *trans* disposed with respect to C3, are much shorter than the Re–P distances in *trans* positions to the carbonyl groups.

This behavior is also noticed for the cationic complexes **4** and **8**, as well as for the neutral derivatives **7** and **9**. In all these derivatives the Re1–P3 distances *trans* to C3, ranging from

(20) Rossi, R.; Marchi, A.; Duatti, A.; Magon, L.; Cesellato, U.; Graziani, R. *J. Chem. Soc., Dalton Trans.* **1988**, 899.

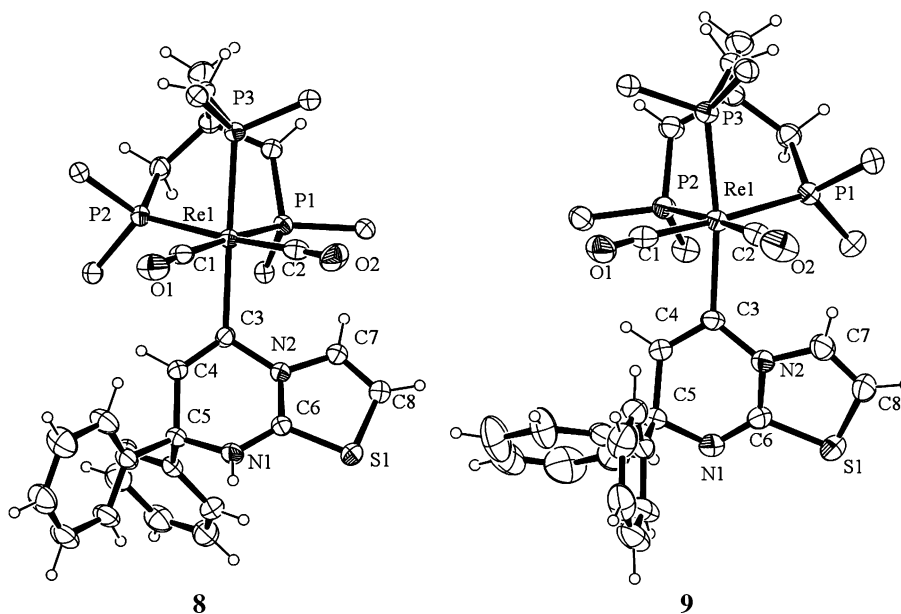
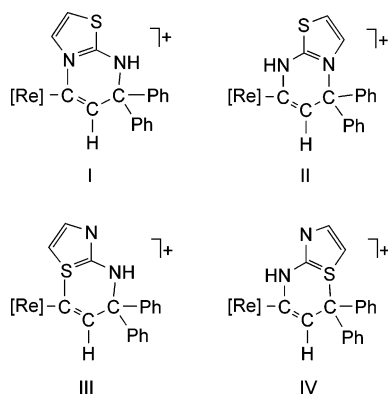
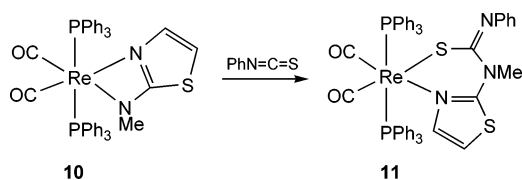


Figure 4. ORTEP view of the complexes of **8** and **9**. The ellipsoids are drawn at the 30% probability level. Only the ipso carbons of the phenyl rings of the triphos ligand are shown for the sake of clarity.

Chart 1



Scheme 10



2.428(2) to 2.446(1) Å, are shorter than the other Re1–P1 and Re1–P2 separations averaging to 2.50 Å on average, thus reflecting the smaller trans influence of these heterocyclic ligands with respect to the carbonyl one. The Re1–C3 distances, ranging from 2.168(3) to 2.239(6) Å, are typical for a Re–C(sp²) single bond as observed in other similar complexes.^{12,14}

In the cation of complex **4**, the triazole ring belonging to the tricyclic ligand exhibits an N2–N3 bond distance of 1.296(2) Å, which is slightly longer than a pure N=N double bond. In the same compound, the N1–N2 and N1–C6 separations, 1.351(3) and 1.363(3) Å, respectively, are only slightly shorter than pure single-bond lengths. Accordingly, the positive charge in these organorhenium compounds can be considered mainly to be localized on the N2 nitrogen and only in part shared with N1. The bicyclic benzotriazole moiety is roughly planar, with maximum deviation from the least-squares plane of 0.023(6) Å for the C6 atom, while the C3–C4–C5–N1–N2 five-

membered ring is not planar, displaying a twisted ³T₄ conformation with the puckering parameters²² $q_2 = 0.053(2)$ Å and $\varphi_2 = 95(3)^\circ$.

In the neutral complex **7** the bicyclic ligand displays a double N1–C6 bond of 1.279(13) Å, giving rise to a perturbation of pyridine aromaticity, as shown by the N2–C6 distance of 1.431(10) Å typical for a C–N single bond and by incomplete π -delocalization within the N2–C7–C8–C9–C10–C6 moiety, which shows alternate longer and shorter bonds. The pyridine ring is almost planar, with a maximum deviation from the mean least-squares plane of 0.06(1) Å for the C6 atom, while the 2*H*-pyrimidine ring N1–C6–N2–C3–C4–C5 is not planar, exhibiting a boat B_{3,6} conformation with the puckering parameters $Q_T = 0.410(8)$ Å, $\varphi_2 = -50.5(7)^\circ$, and $\theta_2 = 80.2(6)^\circ$. The mean least-squares planes passing through the two rings form an angle of 16.5(4)°.

In the cation complex **8** the 2*H*-pyrimidinium group is protonated at the N1 nitrogen. Because the N1–C6 and C6–N2 distances of 1.334(10) and 1.331(11) Å show an extended delocalization through the N1–C6–N2 moiety, the positive charge can be considered equally distributed on both of the nitrogens. The 2*H*-pyrimidinium ring adopts a twisted ³T₁ conformation with the puckering parameters $Q_T = 0.387(6)$ Å, $\varphi_2 = 138.6(9)^\circ$, and $\theta_2 = 106.4(8)^\circ$, while the thiazole ring is almost planar. The mean least-squares planes passing through the two rings make an angle of 10.8(2)°.

Finally, in the deprotonated complex **9** the bicyclic ligand contains three perfect double bonds, C3–C4 = 1.349(7) Å, N1–C6 = 1.276(7) Å, and C7–C8 = 1.332(6) Å, showing the absence of any π -delocalization within the rings. The thiazole derivative is almost planar, with a maximum deviation from the mean least-squares plane of 0.048(5) Å for the C6 atom, while the six-membered ring is not planar, showing a boat B_{3,6} conformation, very similar to that observed for complex **7**, with almost identical puckering parameters: $Q_T = 0.405(5)$ Å, $\varphi_2 = -50.5(7)^\circ$, and $\theta_2 = 80.2(6)^\circ$. The mean least-squares planes passing through the two rings make an angle of 13.4(2)°.

Concluding Remarks

This study has highlighted that the rhenium(I) allenylidene complex [(triphos)(CO)₂Re{C=C=CPh₂}]OTf (**1**) represents a proper platform to build a variety of polyheterocycles by 1,2,3-diheterodicyclization with several N,N-heterocycles containing two nucleophilic nitrogen atoms and one electrophilic hydrogen atom. These include pyrazole, 1*H*-benzotriazole, 2-aminopyridine, and 2-aminothiazole. In all of the cases studied, the condensation between the Re=C=C=C assembly and the heterocycle occurs with complete regioselectivity, yielding cationic organorhenium species featuring bicyclic or tricyclic organyl ligands.

Addition of strong bases such as sodium methoxide readily deprotonates the polycyclic ligands at either the N–H pyrimidine unit (2-aminopyridine and 2-aminothiazole) or the endocyclic vinylic proton (pyrazole, 1*H*-benzotriazole). In the latter case, the deprotonation causes reversible ring opening to yield rhenium alkynyl complexes bearing pyrazolyl or benzotriazolyl substituents on the C_γ carbon. Studies aimed at liberating the polyheterocycles by hydrolysis of the Re–C bonds are planned.

Experimental Section

General Procedure. All reactions and manipulations were routinely performed under a dry nitrogen atmosphere by using standard Schlenk-tube techniques. Tetrahydrofuran (THF) was freshly distilled over LiAlH₄; *n*-hexane was stored over molecular sieves and purged with nitrogen prior to use; dichloromethane and methanol were purified by distillation over CaH₂ before use. The complexes **1**,⁶ **2**,¹⁴ and **3**¹⁴ were prepared as previously reported; 1*H*-benzotriazole, 2-aminopyridine, and 2-aminothiazole were purchased from Aldrich and used without further purification. All the other reagents and chemicals were commercial products and, unless otherwise stated, were used as received without further purification. The solid complexes were collected on sintered-glass frits and washed with diethyl ether or *n*-hexane before being dried under a stream of nitrogen unless otherwise stated. IR spectra were obtained as KBr pellets using a Nicolet 510P FT-IR (4000–200 cm⁻¹) spectrophotometer. Deuterated solvents for NMR measurements (Aldrich and Merck) were dried over molecular sieves (4 Å). ¹H and ¹³C{¹H} NMR spectra were recorded on Bruker AC200, Varian VXR300, and Bruker AVANCE DRX500 spectrometers operating at 200.13, 299.94, and 500.13 MHz (¹H) and 50.32, 75.42, and 125.75 MHz (¹³C), respectively. Peak positions are relative to tetramethylsilane and were calibrated against the residual solvent resonance (¹H) or the deuterated solvent multiplet (¹³C). ³¹P{¹H} NMR spectra were recorded on the same instruments operating at 81.01, 121.42, and 202.46 MHz, respectively. Chemical shifts were measured relative to external 85% H₃PO₄, with downfield values taken as positive. ¹³C{¹H} DEPT-135 NMR experiments were run on the Varian VXR300 spectrometer. ¹H, ¹³C-2D HETCOR NMR experiments were recorded on the Bruker AVANCE DRX 500 spectrometer equipped with a 5 mm triple-resonance probe head for ¹H detection and inverse detection of the heteronucleus (inverse correlation mode, HMQC experiment) with no sample spinning. ¹H, ¹H-2D COSY NMR experiments were conducted on the same instrument. Elemental analyses (C, H, N, S) were performed using a Carlo Erba Model 1106 elemental analyzer.

Synthesis of the Complexes. [(triphos)(CO)₂Re{C=C(H)C(Ph)₂N(C₆H₄)N=N}]OTf (**4-OTf**). A solution of **1** (200.0 mg, 0.17 mmol) in CH₂Cl₂ (10 mL) was treated with a stoichiometric amount of 1*H*-benzotriazole (20.5 mg, 0.17 mmol), and the mixture was stirred at room temperature for 72 h: the color slowly changed from deep violet to dark red. Removal of the solvent in vacuo gave

an orange solid, which was washed with diethyl ether (2 × 3 mL). Yield: 74%. ¹³C{¹H} NMR (75.4 MHz, 293 K, CDCl₃, triphos signals): δ 39.6 (m, CH₃), 39.0 (m, CH₃–C), 35.7 (t, J_{CP} = 13.1 Hz, CH₂–P_{eq}), 32.3 (d, J_{CP} = 24.1 Hz, CH₂–P_{ax}). Anal. Calcd for C₆₅H₅₄N₃O₅F₃P₃ReS: C, 58.91; H, 4.15; N, 3.17; S, 2.41. Found: C, 59.30; H, 4.15; N, 3.22; S, 2.36.

[(triphos)(CO)₂Re{C=C(H)C(Ph)₂N(C₆H₄)N=N}]BPh₄ (**4-BPh₄**). The tetraphenylborate salt was obtained by dissolving **4-OTf** (100.0 mg, 0.07 mmol) in 5 mL of ethanol and adding a solution of NaBPh₄ (51.3 mg, 0.15 mmol) in 5 mL of ethanol. The brown-orange solid that precipitated was filtered out and washed with ethanol (2 × 2 mL) and diethyl ether (2 × 3 mL). The crude product was recrystallized at room temperature from dichloromethane and methanol. Yield: 87%. Anal. Calcd for C₈₈H₇₄N₃O₃BP₃Re: C, 70.68; H, 4.99; N, 2.81. Found: C, 71.02; H, 4.87; N, 2.94.

[(triphos)(CO)₂Re{C≡CC(Ph)₂N(C₆H₄)N=N}] (**5**). A solution of **4-OTf** (200.0 mg, 0.13 mmol) in 10 mL of THF was treated with sodium methoxide (10.3 mg, 0.19 mmol) and stirred at room temperature for 3.5 h. Then the solvent was removed in vacuo, leaving a pink solid that was taken up with CH₂Cl₂ (5 mL) and filtered through Celite. Concentration of the solution to ca. 1 mL and slow addition of diethyl ether (3 mL) gave a pale pink solid, which was washed with diethyl ether (2 × 5 mL) and *n*-hexane (1 × 3 mL). Yield: 78%. ¹³C{¹H} NMR (75.4 MHz, 293 K, CDCl₃, triphos signals): δ 40.3, (q, J_{CP} = 9.7 Hz, CH₃), 39.8 (q, J_{CP} = 4.1 Hz, CH₃–C), 35.3 (d, J_{CP} = 23.3 Hz, CH₂–P_{ax}), 34.0 (td, J_{CP} = 13.7 Hz, J_{CP} = 6.4 Hz, CH₂–P_{eq}). Anal. Calcd for C₆₄H₅₃N₃O₃P₃Re: C, 65.41; H, 4.54; N, 3.57. Found: C, 65.62; H, 4.58; N, 3.51.

In Situ NMR Reaction of 5 with CF₃SO₂OH. A 5 mm screw-cap NMR tube was charged with a degassed solution of **5** (35.2 mg, 0.03 mmol) in 0.7 mL of CD₂Cl₂, and then 1 equiv of CF₃SO₂OH (2.7 μL, 0.03 mmol) was added with a syringe through the serum cap. Immediately the pale pink color changed to deep violet, indicating that **1** forms as soon as the acid is added. ³¹P{¹H} NMR analysis of the sample confirms the complete transformation of **5** into **1**. On standing, **1** may be once more converted back to **4** via slow recombination with the free 1*H*-benzotriazole present in the NMR tube.

[(triphos)(CO)₂Re{C=C(H)C(Ph)₂N(H)C(CH₃)₄N}]OTf (**6**). A solution of **1** (200.0 mg, 0.17 mmol) in 10 mL of CH₂Cl₂ was treated with an excess of 2-aminopyridine (80.0 mg, 0.85 mmol), and the mixture was stirred at room temperature for 3 h. The color slowly changed from dark violet to yellowish orange. The solvent was removed in vacuo, and the residue was washed with diethyl ether (3 × 3 mL) to yield a yellow solid. Yield: 82%. ¹³C{¹H} NMR (75.4 MHz, 293 K, CDCl₃, triphos signals): δ 39.9 (q, J_{CP} = 9.7 Hz, CH₃), 38.5 (q, J_{CP} = 4.1 Hz, CH₃–C), 37.0 (td, J_{CP} = 13.8 Hz, J_{CP} = 5.4 Hz, CH₂–P_{eq}), 32.3 (d, J_{CP} = 22.2 Hz, CH₂–P_{ax}). Anal. Calcd for C₆₄H₅₅N₂O₅F₃P₃ReS: C, 59.12; H, 4.26; N, 2.15; S, 2.47. Found: C, 58.80; H, 4.43; N, 2.02; S, 2.57.

[(triphos)(CO)₂Re{C=C(H)C(Ph)₂NC(CH₃)₄N}] (**7**). A solution of **6** (200.0 mg, 0.15 mmol) in 10 mL of THF was treated with an excess of solid sodium methoxide (17.0 mg, 0.31 mmol) and the mixture stirred at room temperature for 2.5 h. The solvent was removed in vacuo and the pale yellow solid washed in turn with H₂O, 2-propanol, and *n*-hexane (3 mL each). **7** may be recrystallized from CH₂Cl₂/petroleum ether (1:1, v/v) at room temperature. Yield: 78%. ¹³C{¹H} NMR (75.4 MHz, 293 K, CD₂Cl₂, triphos signals): δ 39.9 (q, J_{CP} = 9.2 Hz, CH₃), 38.5 (q, J_{CP} = 2.0 Hz, CH₃–C), 37.3 (td, J_{CP} = 14.2 Hz, J_{CP} = 5.1 Hz, CH₂–P_{eq}), 34.0 (d, J_{CP} = 20.3 Hz, CH₂–P_{ax}). Anal. Calcd for C₆₃H₅₄N₂O₂P₃Re: C, 65.78; H, 4.73; N, 2.43. Found: C, 65.45; H, 5.00; N, 2.40.

Table 4. Crystallographic Data

	3	4	7	8	9
formula	C ₆₁ H ₅₂ N ₂ O ₂ P ₃ Re	C ₆₄ H ₅₄ N ₃ O ₂ P ₃ Re· C ₂₄ H ₂₀ B·CH ₂ Cl ₂	C ₆₃ H ₅₄ N ₂ O ₂ P ₃ Re· 2CH ₂ Cl ₂	C ₆₁ H ₅₃ N ₂ O ₂ P ₃ SRe· C ₂₄ H ₂₀ B·C ₃ H ₇ OH· CH ₃ OH	C ₆₁ H ₅₂ N ₂ O ₂ P ₃ SRe· 1/2CH ₂ Cl ₂
M _r	1124.16	1580.35	1320.04	1568.57	1198.68
space group	<i>Pbca</i>	<i>P</i> $\bar{1}$	<i>P</i> $\bar{1}$	<i>P</i> $\bar{1}$	<i>P</i> $\bar{1}$
cryst syst	orthorhombic	triclinic	triclinic	triclinic	triclinic
a/Å	19.9767(2)	10.7561(1)	13.6973(2)	12.9736(2)	13.7255(2)
b/Å	19.9099(2)	18.3415(2)	14.3060(2)	18.6676(3)	14.2675(2)
c/Å	25.8490(2)	20.4445(2)	17.9666(3)	18.9829(3)	17.4984(3)
α/deg	90	68.8734(4)	70.7666(5)	117.5604(7)	71.0420(6)
β/deg	90	83.3823(4)	78.3629(5)	107.3454(8)	76.4757(7)
γ/deg	90	81.3935(6)	63.8146(8)	93.8150(9)	61.3240(6)
U/Å ³	10 281.0(2)	3711.66(6)	2976.36(8)	3775.1(1)	2830.74(8)
Z	8	2	2	2	2
D _c /g cm ⁻³	1.453	1.414	1.473	1.380	1.406
F(000)	4544	1612	1332	1612	1210
μ(Mo Kα)/cm ⁻¹	25.03	18.26	23.47	17.54	23.59
no. of measd rflns	65 779	53 717	40 784	43 044	43 543
no. of unique rflns	11 790	21 449	13 756	16 234	16 126
R _{int}	0.048	0.042	0.050	0.071	0.047
no. of obsd rflns (I ≥ 2σ(I))	7820	17679	11774	14091	13966
θ _{min} –θ _{max} /deg	2–28	3–30	2–28	3–27	3–30
hkl ranges	–26 to +26; –26 to +26; –34 to +34	–15 to +15; –24 to +25; –28 to +28	–18 to +18; –16 to +18; –22 to +23	–16 to +16; –23 to +23; –24 to +22	–19 to +19; –17 to +20; –23 to +24
R(F ²) (obsd rflns)	0.0426	0.0354	0.0556	0.0562	0.0443
R _w (F ²) (all rflns)	0.1176	0.0814	0.1657	0.1543	0.1137
no. of variables	623	911	681	884	660
goodness of fit	1.157	1.032	1.075	1.189	1.056

In Situ NMR Reaction of 7 with CF₃SO₂OH. One equivalent of CF₃SO₂OH (2.7 μL, 0.03 mmol) was syringed into a CD₂Cl₂ solution (0.8 mL) of **7** (30.0 mg, 0.03 mmol) in a 5 mm screw-cap NMR tube. ³¹P{¹H} NMR analysis showed the complete transformation of **7** into **6**.

[(triphos)(CO)₂Re{C=C(H)C(Ph)₂N(H)CS(CH₂)₂N}]OTf (**8-OTf**). A stoichiometric amount of 2-aminothiazole (17.0 mg, 0.17 mmol) was added to a stirred solution of **1** (200.0 mg, 0.17 mmol) in CH₂Cl₂ (10 mL). The solution was stirred at room temperature for 24 h to give a deep red solution. Concentration under nitrogen to ca. 1 mL and addition of diethyl ether (3 mL) gave **8** as pale orange microcrystals. Yield: 81%. ¹³C{¹H} NMR (75.4 MHz, 293 K, CDCl₃, triphos signals): δ 39.6 (q, J_{CP} = 9.1 Hz, CH₃), 38.4 (q, J_{CP} = 5.0 Hz, CH₃–C), 37.1 (td, J_{CP,eq} = 14.4 Hz, J_{CP,ax} = 5.5 Hz, CH₂–P_{eq}), 32.5 (d, J_{CP,ax} = 21.2, CH₂–P_{ax}). Anal. Calcd for C₆₂F₃H₅₃N₂O₅P₃ReS₂: C, 57.00; H, 4.09; S, 4.91; N, 2.14; S, 4.91. Found: C, 56.82; H, 3.97; N, 2.25; S, 4.91.

[(triphos)(CO)₂Re{C=C(H)C(Ph)₂N(H)CS(CH₂)₂N}]BPh₄ (**8-BPh₄**). The tetraphenylborate salt **8-BPh₄** can be obtained by dissolving **8-OTf** (100.0 mg, 0.08 mmol) in 5 mL of ethanol and adding a solution of NaBPh₄ (54.7 mg, 0.16 mmol) in 5 mL of ethanol. The orange solid that precipitated was filtered out and washed with ethanol (2 × 2 mL) and diethyl ether (2 × 3 mL). **8-BPh₄** was crystallized at room temperature from CH₂Cl₂/2-propanol. Yield: 80%. Anal. Calcd for C₈₅H₇₃N₂O₂BF₃P₃ReS: C, 69.14; H, 4.98; N, 1.90; S, 2.17. Found: C, 70.02; H, 5.06; N, 1.94; S, 2.32.

[(triphos)(CO)₂Re{C=C(H)C(Ph)₂NCS(CH₂)₂N}] (**9**). A solution of **8-BPh₄** (200.0 mg, 0.13 mmol) in 10 mL of THF was treated with sodium methoxide (14.6 mg, 0.27 mmol) and stirred at room temperature for 3.5 h. Afterward, the solvent was removed in vacuo and the solid was redissolved in CH₂Cl₂ (5 mL) and filtered through Celite. Concentration of the solution to ca. 1 mL and slow addition of diethyl ether (3 mL) gave a beige solid, which was washed with diethyl ether (2 × 5 mL) and *n*-hexane (1 × 3 mL). **9** was

crystallized at room temperature from dichloromethane and diethyl ether. Yield 83%. ¹³C{¹H} NMR (75.4 MHz, 293 K, CD₂Cl₂, triphos signals): δ 40.2 (q, J_{CP} = 11.8 Hz, CH₃), 39.3 (q, J_{CP} = 2.4 Hz, CH₃–C), 38.2 (td, J_{CP,eq} = 13.4 Hz, J_{CP,ax} = 6.1 Hz, CH₂–P_{eq}), 34.9 (d, J_{CP,ax} = 19.5 Hz, CH₂–P_{ax}). Anal. Calcd for C₆₁H₅₂N₂O₂P₃ReS: C, 63.36; H, 4.50; N, 2.42; S, 2.77. Found: C, 63.54; H, 4.83; N, 2.29; S, 2.81.

In Situ NMR Reaction of 9 with CF₃SO₂OH. One equivalent of CF₃SO₂OH (2.7 μL, 0.03 mmol) was syringed into a CD₂Cl₂ solution (0.8 mL) of **9** (30.0 mg, 0.03 mmol) in a 5 mm screw-cap NMR tube. ³¹P{¹H} NMR analysis showed the complete transformation of **9** into **8**.

X-ray Structure Determinations. Crystal data for compounds **3**, **4**, and **7–9** were collected on a Nonius Kappa CCD diffractometer using graphite-monochromated Mo Kα radiation (λ = 0.7107 Å) at room temperature (295 K). Data sets were integrated with the Denzo-SMN package²³ and corrected for Lorentz–polarization and absorption effects.²⁴ The crystal parameters and other experimental details of the data collections are summarized in Table 4. The structures were solved by direct methods (SIR97)²⁵ and refined by full-matrix least-squares methods with all non-hydrogen atoms anisotropic and hydrogens included on calculated positions, riding on their carrier atoms. All calculations were performed using SHELXL-97²⁶ and PARST²⁷ implemented in the WINGX system of programs.²⁸ ORTEP²⁹ views are shown in Figures 1–5. Selected bond distances and angles are given in Tables 2 and 3.

(23) Otwinowski, Z.; Minor, Z. In *Methods in Enzymology*; Carter, C. W., Sweet, R. M., Eds.; Academic Press London, 1977; Vol. 276, Part A, pp 307–326.

(24) Blessing, R. H. *Acta Crystallogr., Sect. A* **1995**, *51*, 33.

(25) Altomare, A.; Burla, M. C.; Camalli, M.; Cascarano, V.; Giacovazzo, C.; Guagliardi, A.; Moliterni, A. G.; Polidori, G.; Spagna, R. *J. Appl. Crystallogr.* **1999**, *32*, 115.

(26) Sheldrick, G. M. SHELXL97, Program for Crystal Structure Refinement; University of Göttingen, Göttingen, Germany, 1997.

(27) Nardelli, M. *J. Appl. Crystallogr.* **1995**, *28*, 659.

(28) Farrugia, L. J. *J. Appl. Crystallogr.* **1999**, *32*, 837.

(29) Burnett, M. N.; Johnson, C. K. *ORTEP-III: Oak Ridge Thermal Ellipsoid Plot Program for Crystal Structure Illustrations*; Report ORNL-6895; Oak Ridge National Laboratory: Oak Ridge, TN, 1996.

Acknowledgment. We wish to thank the COST Action D17/003 of the European Community for promoting this scientific activity. M.P. thanks “Firenze Hydrolab”, a project sponsored by the ECRF, for the use of the NMR instrument. I.R. thanks the Spanish “Ministerio de Educacion y Cultura” for a Ramon y Cajal contract.

Supporting Information Available: X-ray crystallographic data in CIF format. This material is available free of charge via the Internet at <http://pubs.acs.org>.

OM050663V